Laser beam attenuation in LIF measurements on NO in a diesel engine

K. Verbiezen[1,*], A.J. Donkerbroek[1], A.P. van Vliet[1], W.L. Meerts[1], R.J.H. Klein-Douwel[2], N.J. Dam[1], and J.J. ter Meulen[1]

[1] Applied Physics Group, University of Nijmegen
Toernooiveld 1, 6525 ED Nijmegen, NL

[2] Mechanical Engineering, Eindhoven University of Technology
P.O. Box 513, 5600 MB Eindhoven, NL

Abstract
The effect of laser beam attenuation on nitric oxide measurements in a diesel engine is presented. A number of experimental ways to correct for this attenuation are discussed: transmission measurements, bidirectional laser-induced fluorescence, and Raman scattering by N_2. Comparison of the results indicates that the attenuation is generally not uniform over the cylinder. Instead it seems to be less severe over the field of view (i.e. the upper part of the cylinder).

Introduction
Diesel engines are used world-wide because they are powerful and economic power sources. One of their less favourable aspects, however, is the strong emission of soot and toxic gases, like nitric oxides (NO_x). There is an ever stronger demand for cleaner diesel engines, because legislation on pollutant emissions is becoming stricter. Detailed knowledge about the combustion process inside the engine is a prerequisite for a systematic approach to cleaner diesel combustion. The objective of this research project is to use laser-based diagnostics for studying spatial and temporal distributions of NO and soot inside the combustion chamber of a realistic diesel engine. The non-intrusiveness of this technique is one of its main advantages. Furthermore, it can be applied within the harsh environment of diesel combustion.

Previous in-cylinder measurements on nitric oxide (NO) conducted in our diesel engine made clear that the laser beam is strongly attenuated by the cylinder contents [1]. This unknown attenuation makes quantitative interpretation of the obtained NO fluorescence distributions difficult.

Several options will be discussed below for studying the attenuation experienced by a (laser) light beam traversing the engine's combustion chamber. Most straightforwardly, the total transmission through the cylinder can be measured as function of time and position. However, this only yields the integrated extinction. Spatial information of the attenuation along the laser beam trajectory is still lacking.

Another option is to illuminate the cylinder (quasi-) simultaneously with two laser beams, traversing the same probe volume but in opposite directions. Recording the scattered light from each laser pulse separately, the *local* attenuation can be calculated [2]. Due to certain limitations, simultaneous measurements were not possible. Only averaged images for both directions can be compared. This indicates qualitatively whether the laser is attenuated over the field of view.

Finally, Raman scattering by N_2 can be detected. Non-reacting in combustion processes, the amount of N_2 is constant. Assuming N_2 to be distributed uniformly (thereby neglecting spatial temperature variations), the scattered light intensity is proportional to the local laser intensity only. On its way out of the combustion chamber, however, this scattered light may be attenuated too. The detected Raman signal has suffered both types of attenuation. Therefore the Raman measurements provide a clue for the attenuation of both the incident laser beam and the scattered light.

Specific Objectives
The ultimate goal of this research is to develop the NO-LIF technique to a level at which *quantitative* NO measurements are possible in a heavy-duty diesel engine. This requires (amongst others) knowledge of the local laser intensity. Therefore, more specifically, several methods are being investigated to deal with laser beam attenuation.

Experimental Setup
All measurements have been performed on a heavy-duty, six-cylinder truck engine (DAF, block of the 1160 series, cylinder head WS268L). Although a number of changes have been made to make it optically accessible, it has been kept as realistic as possible. One of the cylinders was fitted with the piston head of a more modern DAF 95XF engine and is used for the *in situ* measurements. It features an eight-hole fuel injector that can be rotated, which allows measurements at different positions relative to the fuel sprays without repositioning the laser beam. Quartz windows were mounted in the cylinder on various places (see figure 1):

* Corresponding author: kasperv@sci.kun.nl
Proceedings of the European Combustion Meeting 2003

there are three windows at the sides, giving a view to the uppermost part of the combustion chamber. In addition, one of the exhaust ports was replaced by a cylindrical window. Finally, there is a big window (70 mm diameter) in the piston bowl (slightly reducing the compression ratio) that enables an upward view into almost the complete chamber. A slot machined into the piston crown prevents complete blocking of one of the side windows even at Top Dead Centre (TDC). No lubricants are used since they absorb the UV laser radiation; to avoid overheating the measurement cylinder is skip-fired. Steady-state conditions are mimicked by (pre-)heating the cooling water to operational temperatures. Details of the modified cylinder and the engine characteristics will be published elsewhere, and can also be found in [1].

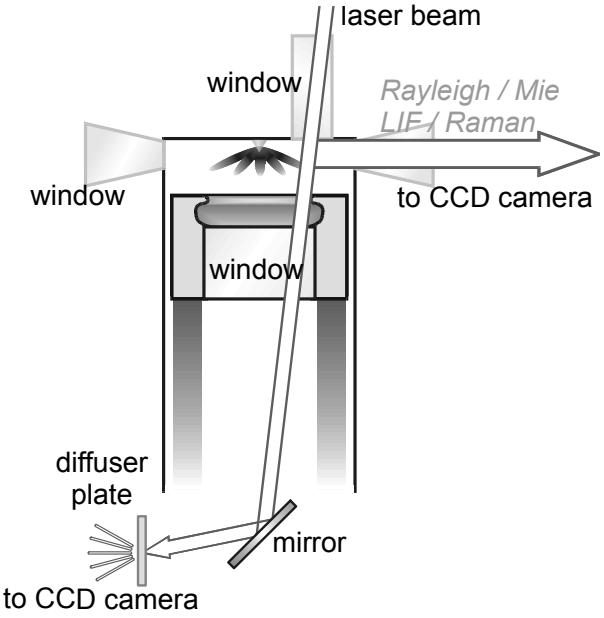

figure 1: Schematic view of the setup

Nitric oxide was detected by means of laser-induced fluorescence (LIF), exciting the NO molecules from the electronic ground state $X\ ^2\Pi(v''=0)$ state) to the $A\ ^2\Sigma(v'=0)$ state. The $Q_1+P_{21}(13)$ and $R_2(15)$ transitions were induced by laser radiation at 226.073 nm. The fluorescence back to several vibrational levels in the electronic ground state (v" = 0, 1, 2 ...) was recorded.

An unfocussed 226 nm laser beam of 2.5 mJ pulse energy entered the chamber by the top window of the measurement cylinder. The laser radiation was produced by a frequency-doubled dye laser (Lambda Physik ScanMate 3 using Coumarin 47) pumped by a Nd:YAG laser (Continuum PowerLite 9010). The scattered light was detected through the side window by an intensified CCD camera (Roper Scientific, ICCD 512T, 16 bits) mounted behind a spectrograph (ARC SpectraPro 500i). The field of view was determined by the diameter of the incident laser beam, and the height of the side window (23 mm). The grating spectrograph projected this field of view onto different positions of the camera chip, resulting in several (sub-) images. The position of each sub-image is determined by the wavelength components in the scattered light. This way, the fluorescence bands from NO and the Mie scattering by soot could be spectrally separated. Of course the Mie scattering, Rayleigh scattering, and the resonant fluorescence could not be distinguished, being all at 226 nm. Since Mie scattering is far stronger than the other two processes, the sub-image at 226 nm will be interpreted as Mie scattering only. In addition, NO-LIF and Mie images were measured with opposite laser beam direction (i.e. bottom-up.

For the overall transmission measurements a quartz diffuser plate was placed in front of the mirror below the piston window. The ICCD camera was directed towards the piston mirror, collecting the laser radiation that was scattered by the diffuser plate. The measurement cylinder was alternatingly non-fired and fired. For two subsequent images the laser intensity was integrated over space and these numbers were divided to yield the transmission.

The Raman measurements were performed using the 355 nm radiation of a frequency-tripled Nd:YAG laser by Spectron Lasers (SL 8354 YDA), at about 210 mJ pulse energy. The laser beam had the same trajectory as for the NO and transmission measurements. An ARC SpectraPro 300i spectrograph was used with the camera mentioned above. Raman scattering is not resonant, thereby enabling (simultaneous) multi-species detection through the side window.

Results and Discussion

All measurements presented here were conducted at one specific set of operation conditions: the engine was run at 1430 rpm, at a load of 10% (fuel injection from 5° bTDC till 6° aTDC). For the bidirectional NO-LIF experiments the laser was directed through the spray path only, whereas the other measurements were also performed between two adjacent sprays.

Fuel spray images

The piston window gives a good view into the combustion chamber. Two images of the natural emission of the flames are shown below (figure 2), one during fuel injection, the other somewhat later in the cycle. The fuel injector is located at the centre of the images. No laser illumination was used.

At 6° aTDC eight fuel sprays are visible, along with their flames (a little further from the centre). Due to the swirl of the intake air, the flames are rotated clockwise with respect to the sprays. Not all flames are equally bright. Although the flame intensities at a certain crank angle may vary from cycle to cycle, the flame near the piston slot (i.e. at four o' clock) is always relatively bright.

The emitted light is spectrally dominated by the broadband radiation of glowing soot, although peaks of OH (308 nm) and CH (431 nm) radicals have been seen as well at 3° aTDC. There is no difference in the spectra from the flame and from the spray. The sprays do not

emit light of their own, they merely reflect the flame luminosity.

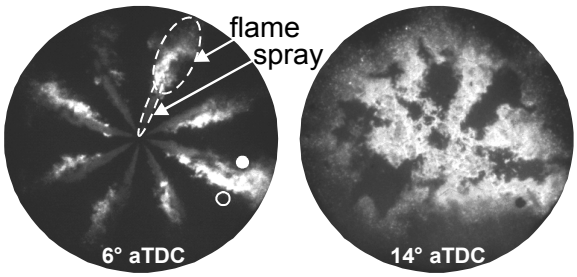

figure 2: Natural luminosity (single-shot) from (combusting) diesel sprays (viewed through the piston window), at 6° aTDC (left) and 14° aTDC (right). A grey-scale is used for the intensity, brighter shades representing higher intensities. The two probe positions are indicated by a white dot (in spray) and an open circle (between sprays).

At 14° aTDC, the whole structure is more homogeneous, although some "islands" of lower luminosity are often present at the original spray locations. Apparently, the cylinder contents are gradually being mixed.

Most of the laser experiments were conducted at two probe positions; both in the spray path (marked by the white dot in the left part of figure 2) and between two sprays (open circle).

Transmission measurements

Transmission curves have been measured for both laser positions. The results are given in figure 3, together with the in-cylinder pressure curve (solid grey line). For both curves the transmission drops drastically during early combustion but for larger crank angles it increases to ~80% of its initial value.

The pressure increase at around 4° aTDC marks the start of combustion (the first ignition spots are visible through the piston window at 3° aTDC). Between the sprays (grey dots) the cylinder is transparent until 10° aTDC, but drops to about 0.1% at 15° aTDC. At this time, combustion has already started. In this position therefore, soot and hot CO_2 appear to be the major cause of laser attenuation [3].

When probing in the spray path, however, this drop starts much earlier (open circles): at 1° aTDC, which is when the fuel spray hits the laser beam. This suggests that the laser beam is initially attenuated (or perhaps merely scattered) by the fuel droplets. After fuel injection has ceased, it is probably the soot that attenuates the laser beam. However, the swirl moves the flames away from the probe volume, hence the earlier increase of the transmission. The graphs are clearly different between 15° and 40° aTDC. This may suggest that hot CO_2, which is expected to be distributed more homogeneously than the soot, hardly contributes to the attenuation. CO_2 starts to absorb 226 nm radiation at temperatures around 1600 K [3], while the average in-cylinder temperature does not exceed 1200 K at these working conditions. Therefore, the CO_2 in the combustion chamber may simply be too cold to absorb.

The absorption by CO_2 strongly decreases with increasing wavelength, reaching a minimum for wavelengths around 250 nm and higher. The contribution of CO_2 to the extinction was also investigated by transmission measurements using radiation at 237 nm (which can be used for probing the $X\ ^2\Pi(v" = 1)$ state of NO). Still, no differences were found in the transmission curves at 226 nm and 237 nm, suggesting negligible absorption by CO_2.

From 40° aTDC onwards the transmission is identical for both positions. Because of the reasonably homogeneously mixed cylinder contents the transmission is no longer position-dependent, as can be seen from the natural flame luminosity images.

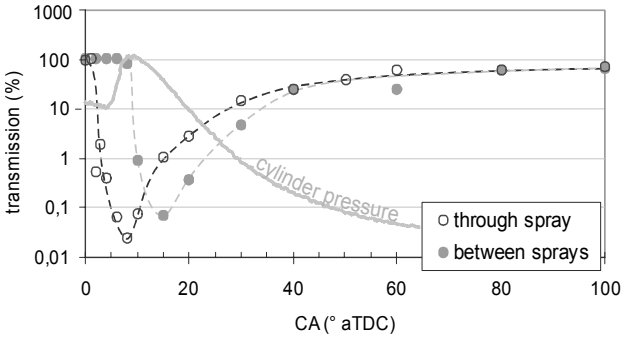

figure 3: Total (vertical) transmission, either through a spray (open circles) or between two sprays (solid grey dots). The dashed lines are drawn to guide the eye. Note the logarithmic ordinate. The solid grey line represents in-cylinder pressure. Although the absolute scale is not shown for the pressure curve, a maximum pressure of 6 MPa is reached.

NO-LIF measurements

The NO-LIF images were recorded through the side window, showing the uppermost 23 mm of the combustion chamber. Two results are displayed in figure 4, taken at 18.5° (upper panel) and 72.5° aTDC (lower panel). In both images the laser beam entered from the top. Because of the spectrograph the scattered light is seen as a series of sub-images (illustrated by grey rectangles in the bottom image), each featuring spatial information on NO or soot. Despite the slot in the piston crown, at 18.5° aTDC the side window is still partially blocked, which explains why the sub-images at 18.5° aTDC are shorter.

Mie scattering by soot (i.e. elastic scattering) can be seen on the extreme right of the image, at 226 nm. The intense "disc" at the top of the sub-image is also present under non-firing conditions and is caused by a reflection off the top window. NO-LIF is visible at 237 nm, 248 nm, and 259 nm, corresponding to the (0,1), (0,2), and (0,3) transitions, respectively. Note that all NO

images originate from the same NO distribution, namely those molecules in the $X\ ^2\Pi(v'' = 0)$ state.

These NO images contain raw data. They need to be processed, correcting for the Boltzmann factor, excitation efficiency, non-radiative decay, and attenuation of both the laser beam and the fluorescence. In this paper, attention will be paid to laser beam attenuation only, neglecting the other corrections.

One aspect of figure 4 that catches the attention is the difference in structure between the LIF and Mie sub-images: the NO seems to be quite uniformly distributed (especially in the lower image) while the soot images are far from uniform. Irregular "blobs" of (probably) soot are clearly visible. Still, these irregularities in soot density are not reflected at all in the NO images, leading to the conclusion that Mie scattering is not a good measure for laser beam attenuation. Either the attenuation is not caused by soot (at least in the field of view), or the Mie scattered light is not proportional to the local extinction factor.

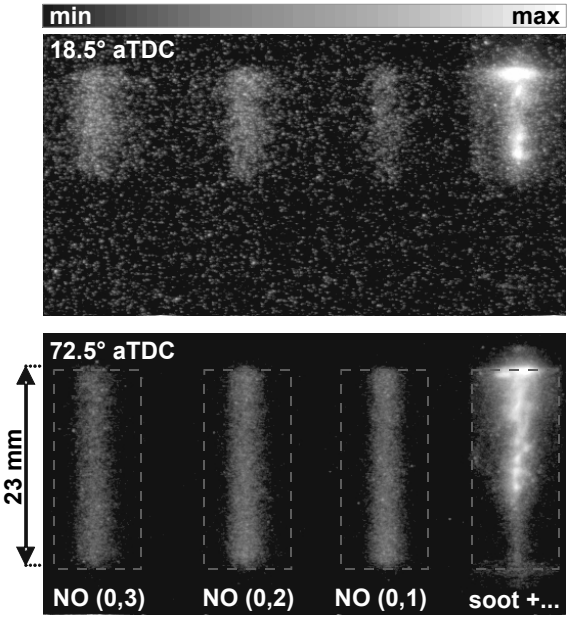

figure 4: Spatial distributions of three fluorescence bands of NO (left) and Mie scattering by soot (extreme right), spectrally separated (see grey dashed rectangles in the lower panel). The images (averages of 10 single shot images are shown here) were recorded through the side window at 18.5° aTDC (upper panel) and 72.5° aTDC (lower panel).

The laser attenuation can be investigated *qualitatively* by the bi-directional NO-LIF experiments. Quantitative study of the attenuation was not performed due to noise on the data. Calculating the attenuation from the two images will blow up the noise to such an extent that interpretation becomes impossible. At present, algorithms are being investigated that can handle the noise.

Figure 5 displays vertical fluorescence profiles for both laser directions (open circles: top-down; grey dots: bottom-up) at 42.5° aTDC. The profiles are obtained by integrating the NO fluorescence for each horizontal image strip. At this crank angle, cycle-to-cycle variations are much smaller than in early combustion. After averaging over ten images (twenty for the bottom-up measurements, where the signal is weaker) a reasonably stable average is obtained, so that the two profiles can be compared.

Apart from a difference in intensity, the vertical profiles are very similar. This indicates that there is hardly any attenuation of the laser beam over the field of view. At 42.5° aTDC the overall transmission is still only 24%, as can be seen in figure 3. In the case of uniform attenuation, this would imply a mere 50% transmission over the field of view, which is certainly not reflected in the NO-LIF profiles. The virtually identical curves in figure 5 can only be explained by non-uniform attenuation, the main laser beam extinction apparently taking place *below* the side window. To illustrate this, uniform transmission profiles (solid lines) are shown in figure 5. The profiles have been scaled by an arbitrary value so as to give a best possible fit to the fluorescence profiles. These curves show what the NO-LIF profiles should look like *if* the NO density and the laser attenuation both were to be uniformly distributed.

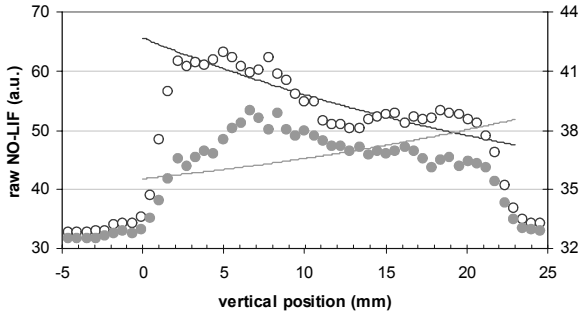

figure 5: Vertical NO-LIF intensity profiles for top-down (open circles) and bottom-up (grey dots) measurements, taken at 42.5° aTDC. Each dot corresponds to an average of 10 neighbouring image strips. The abscissa represents the vertical position: 0 mm corresponds to the top of the side window, 23 mm to the bottom. The profiles are 10 shot averages (20 shots for bottom-up). Note the different scale (at the right side) for the bottom-up profile. The NO-LIF intensities are lower for the bottom-up experiments.

N_2 Raman measurements

Raman scattering by both N_2 and O_2 has been observed in the engine. Early in the stroke the Raman signature of probably hydrocarbons can be observed as well, but that will not be discussed further here. The O_2 (sub-) image is of no use for investigating laser beam attenuation. It does allow, however, to determine the local O_2/N_2 ratio, even on a single-shot basis, yielding important

parameters of the combustion process. Unfortunately the O_2 signal is weaker, which results in small signal-to-noise ratios, especially later in the stroke.

Three typical Raman images are shown in figure 6, recorded at TDC, 6° aTDC, and 20° aTDC. These measurements were done in the spray path (figure 2, solid circle). The images have been processed to remove the broadband background radiation, caused by laser-induced incandescence (and maybe some LIF by polycyclic aromatic hydrocarbons, PAHs).

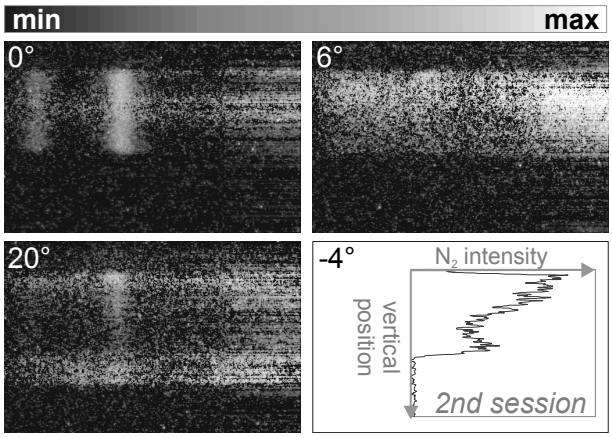

figure 6: Raman images (averages of twenty shots) taken through the side window, at TDC (top left), 6° aTDC (top right), and 20° aTDC (bottom left). Scattering by N_2 (and O_2) is clearly visible before start of combustion, but also again at 20° aTDC. A vertical intensity profile of N_2 is displayed bottom right. Recorded after the other three images, the profile at 4° bTDC clearly shows the effect of dirt on the side window.

At TDC, the N_2 and O_2 images are uniform. At this time, the fuel spray has not yet reached the probe volume, and combustion has not started. At 6° aTDC the N_2 signal vanishes, except perhaps for the uppermost 3 mm. During the subsequent 12° CA, the N_2 image is slowly growing and increasing in strength, but only at 20° aTDC it is visible again over the complete field of view. Somewhat below the middle the N_2 signal is weaker, but that is due to fouling of the side window. To illustrate this, a vertical intensity profile of N_2 is added in the lower right panel of figure 6. The corresponding measurement was taken *after* the other images, at a crank angle of 4° bTDC, when the engine is still transparent. Clearly, the profile is not flat, while the intensity minima of the profile and the image at 20° aTDC correspond well.

To study the time dependence of the N_2 signal, the total intensity of the N_2 sub-image is plotted for a series of crank angles. The N_2 values were corrected for cylinder compression and also for blocking of the side window by the piston during earlier crank angles. This way the processed values represent the laser intensity, averaged over the field of view. Temperature inhomogeneities were not taken into account. The results are plotted in figure 7 as open circles, for both probe positions. The data point for 4° aTDC lies above the upper limit of the graph; it will not be discussed here. As a comparison, the field-of-view averaged transmission was also calculated from the transmission data assuming uniform attenuation (displayed as grey dots in figure 7).

Probing through a spray (upper panel), there are some differences between the curves. While the transmission drops at 1° aTDC (which is when the spray has reached the probe volume), the N_2 Raman signal is visible until 6° aTDC. Even when the fuel spray hits the laser beam, the N_2 signal is still present, while the overall transmission drops rapidly (figures 3 and 7). Apparently the low transmission around 2° aTDC is due to scattering of the laser beam by the fuel spray. The N_2 Raman signal recovers more steeply than the transmission, indicating that the attenuation is not uniform, but instead more localised below the field of view, i.e. the bottom of the cylinder.

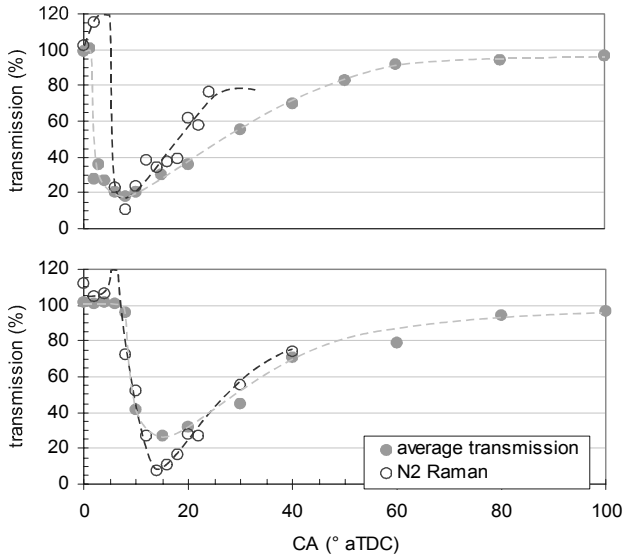

figure 7: Integrated N_2 Raman intensity as a function of crank angle (open circles), both in the spray (upper panel) and between sprays (lower panel). The grey dots represent the laser intensity at the side window, based on the transmission data and assuming uniform attenuation. Dashed lines were added to both curves as a guide for the eye.

Between the sprays (lower panel), both curves agree well. It seems that the attenuation is indeed uniform in this position. In general, such mono-exponential decay of the laser intensity is reflected by the vertical N_2 Raman profiles (not shown here). Due to their low signal-to-noise ratio around 20° aTDC, this could only be verified for measurements at 30° and 40° aTDC.

In principle, the Raman results yield quantitative intensity values that do not only incorporate the laser beam attenuation, but also the attenuation of the scattered light on its way to the camera. Therefore,

division of integrated NO-LIF values by the corresponding N_2 correction factor will yield a correction for both laser beam attenuation and fluorescence attenuation at the same time. This method does, of course, involve the assumption that the attenuation of 355 nm and 226 nm radiation behaves similarly. Note also that the NO and N_2 number densities have the same temperature dependence. Division will yield a quantity comparable to the *mole fraction* [4]. This quantity is independent of attenuation, because the latter is divided out.

Conclusions

We have shown that laser beam attenuation can be quite strong in a diesel engine: at certain crank angles, the intensity is diminished by at least a factor of 1000. The exact value of this factor strongly varies with crank angle, and is also position-dependent.

Comparison of simultaneously detected NO-LIF and Mie scattering images show that the Mie distributions are far more irregular. Since they are not reflected in the NO sub-images, these structures do not seem to contribute to the laser beam attenuation at all. The bidirectional NO-LIF experiments suggest that at 42.5° aTDC the laser beam attenuation over the field of view is much lower than the transmission data tell. In principle, this bidirectional method is the best way to *quantitatively* reconstruct the local laser intensity. Unfortunately, the reconstruction algorithm is still too sensitive to noise, but several methods are being investigated to deal with this problem.

The N_2 Raman measurements offer an interesting alternative. An advantage over the bidirectional fluorescence method is that the attenuation of the scattered light is corrected for as well. Near the spray flames, temperature and hence density gradients limit the interpretation of the local laser intensity. Further away, and later in the combustion stroke, these gradients will be much smaller, if not negligible. If density variations cannot be ignored, the corrected NO signal may be interpreted as the local NO/N_2 ratio.

The combined transmission and Raman scattering data indicate that the initial drop in laser beam transmission (when probing through the spray) may largely be due to scattering rather than to absorption. The steeper increase of the N_2 Raman intensity between 16° and 24° aTDC suggests that the major laser beam attenuation takes place below the field of view. Between the sprays, the attenuation seems to be more uniform, as could be confirmed by the vertical N_2 Raman intensity profiles at 30° and 40° aTDC, that indeed show an exponential decay.

Acknowledgements

The authors are grateful to STW, the Applied Science Division of the Nederlandse Organisatie voor Wetenschappelijk Onderzoek,, for their financial support. Special thanks go out to R.S.G. Baert and T. Gerber for their fruitful collaboration.

References

[1] H.L.G.J. van den Boom, Ph.D. Dissertation, University of Nijmegen, Nijmegen, the Netherlands (2000)

[2] G.G.M. Stoffels, S. Stoks, N.J. Dam, J.J. ter Meulen, Applied Optics 39, 5547-5559 (2000)

[3] F. Hildenbrand, C. Schulz, F. Keller, G. König, E. Wagner, SAE paper No. 2001-01-3500 (2001)

[4] J. Warnatz, U. Maas, R.W. Dibble, Combustion, Springer-Verlag, Berlin Heidelberg, 1996